

(0^+ , 1^-) state at 16.35 MeV and a 2^+ ; $T=1$ state at 16.44.⁶ Our data cannot be fit with an $L=0$ distribution. Both, $L=1$ and $L=2$ distributions are fairly consistent with the cross section data whereas the $L=1$ description is slightly better for the analyzing power data.

The overall reproduction of the data by DWBA is similar for $^{17}\text{O}(p,t)$ and $^{18}\text{O}(p,t)$ for the known configurations in the final nuclei. The question whether the zero-range approximation or the finite-range DWBA code or perhaps both develop serious problems at large momentum mismatch is still under investigation.

[†]Present address: Physics Department, Princeton University, Princeton, NJ 08544

- 1) W.W. Daehnick et al., IUCF Annual Report 1983, p.94 K.F. v. Reden et al., to be submitted for publication.
- 2) M. Pignanelli et al., Phys. Rev. C 8, 2120 (1973).
- 3) M. Pignanelli et al., Phys. Rev. C 10, 445 (1974).
- 4) Proton elastic scattering on ^{17}O - this experiment.
- 5) H. Nann et al. - private communication: $\text{natO}(^3\text{He}, ^3\text{He})$ at 78.6 MeV, IUCF 1984.
- 6) F. Ajzenberg-Selove, Nucl. Phys. A375 (1982).

ENERGY DEPENDENCE OF THE $^{24}\text{Mg}(p,d)$ REACTION FOR VARIOUS ℓ TRANSFERS

D.W. Miller, J.D. Brown[†], D.L. Friesel, W.W. Jacobs, W.P. Jones, H. Nann, P. Pichardo
Indiana University Cyclotron Facility, Bloomington, Indiana 47405

J.Q. Yang
Institute of Nuclear Research, Academia Sinica, Shanghai, China

P.W.F. Alons and J.J. Kraushaar
University of Colorado, Boulder, Colorado 80309

Early analyses¹ of results of (p,d) reaction cross-section and analyzing-power measurements obtained for $\ell = 0$ transitions raised substantial questions regarding the applicability of standard DWBA methods to this reaction at or above 100-MeV bombarding energy. The purpose of the present investigation was to study transitions involving different orbital angular momentum (ℓ) and spin (j) transfers as a function of bombarding energy to provide a data base for detailed theoretical investigations of the energy dependence of the reaction mechanism.

Measurements of cross-section and analyzing-power angular distributions were carried out using the same detector telescope at bombarding energies of 49.2 and 150.3 MeV for the $^{24}\text{Mg}(p,d)$ reaction to the known

low-lying $J^\pi = 1/2^+$, $1/2^-$, $3/2^-$, $3/2^+$, $5/2^+$, and $7/2^+$ residual states of ^{23}Mg . A few data points were also taken at 95 MeV in order to provide a cross normalization of the telescope results with earlier 95-MeV spectrometer measurements.^{2,3} An analysis of the distributions for the lowest $1/2^+$ state, incorporating results from a number of other laboratories spanning the bombarding-energy range from 27 to 185 MeV, has already been published.⁴

The telescope consisted of five elements, a 2-mm thick Si surface barrier detector followed by 12.0, 13.0, 9.4 and 13.0-mm thick intrinsic Ge detectors. The overall (full width at half maximum) resolution of the system including target thickness, kinematic spread, and the detector stack plus electronics was about

200 keV at 49.2 MeV and 300 keV at 150.3 MeV. Although some deuteron groups were not well resolved at 150 MeV, locations of the residual states were well known, and reliable peak fitting was achieved for all the cases reported here. The absolute cross sections are estimated to have an uncertainty of $\pm 15\%$ at 49.2 MeV and $\pm 25\%$ at 150.3 MeV, the latter due to uncertainty in the telescope efficiency.

Results were obtained for groups leading to the two $1/2^+$ states (2.36 and 4.36 MeV), as well as to the low-lying $1/2^-$ (2.77 MeV), $3/2^-$ (3.80 MeV), $3/2^+$ (ground state), $5/2^+$ (0.45 MeV) and $7/2^+$ (2.05 MeV) states. Plots of the results for the $1/2^+$ state at 2.36 MeV as a function of angle have already been published.⁴ It should be noted that the main oscillatory features of both cross sections and analyzing powers for the $\ell = 0$ transitions are reasonably stable when plotted against angle, but shift substantially when plotted against momentum transfer for the data at different bombarding energies.

Figures 1-3 present the cross-section and analyzing-power distributions for groups leading to all but the $1/2^+$ states at 49.2, 94.8 and 150.3 MeV bombarding energy, plotted as a function of momentum transfer q for comparison. Results for the $1/2^-$ and $3/2^-$ states, assumed to be dominated by a one-step $\ell = 1$ transfer, are shown in Fig. 1. The most striking j -dependent feature of the analyzing powers (predominately negative values for $1/2^-$ states at forward angles compared to the near zero values for $3/2^-$ states)^{3,5} which appears to be nearly stable with angle at around $\theta_{\text{cm}} = 8^\circ$, clearly shifts when the data are plotted against momentum transfer. However, the larger-angle oscillations in the analyzing powers shift when plotted versus either θ_{cm} or q . For the $\ell = 2$ transfer results ($3/2^+$ and $5/2^+$ states) plotted in Fig. 2, the j -dependence is less pronounced. Figure 3 shows the results for the $7/2^+$ state at 2.05 MeV, which is presumed to be excited primarily by a two-step mechanism.

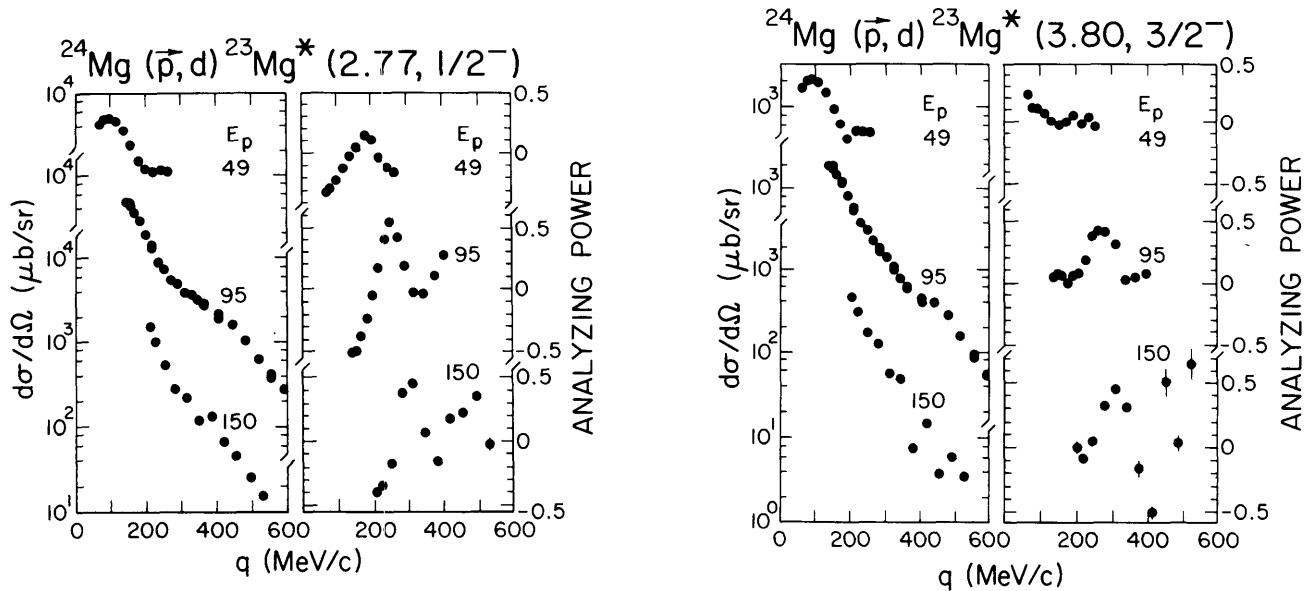


Figure 1. (p, d) differential cross section and analyzing-power angular distributions for two $\ell = 1$ transitions to low-lying states in ^{23}Mg as a function of bombarding energy. Present telescope results at 49.2 and 150.3 MeV are plotted at the top and bottom, with the previously-published spectrometer results at 94.8 MeV in the center.

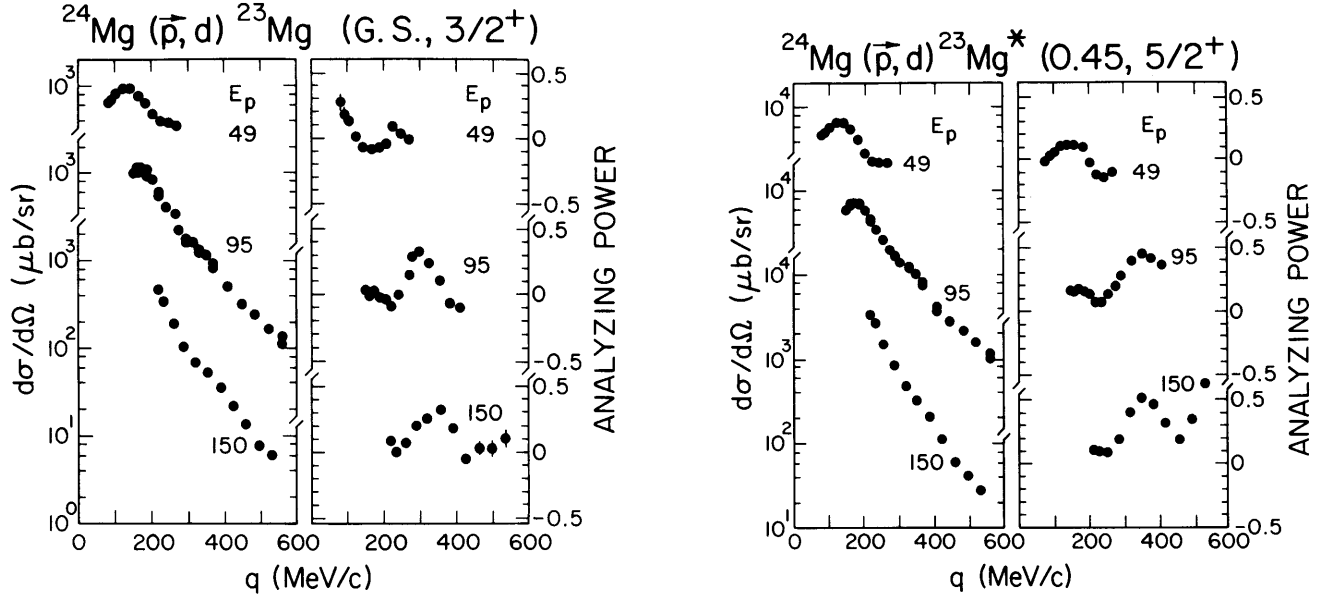


Figure 2. (p,d) differential cross section and analyzing-power angular distributions for two $\ell = 2$ transitions to low-lying states in ^{23}Mg .

Exact finite-range distorted-wave calculations have been carried out using the code⁶ FRUCK2 applying the adiabatic approximation.⁷ The standard bound-state geometry with radius 1.25 fm and diffuseness 0.65 fm was employed, with the spin-orbit parameter $\lambda = 25$. Proton optical-model parameters at 49, 95 and 150 MeV were obtained from the prescription of Hatanaka et al.⁸

Figures 4 and 5 show $\ell = 1$ and $\ell = 2$ comparisons between the data, plotted as a function of θ_{cm} , and the distorted-wave predictions using the Hatanaka prescription throughout. This prescription extrapolated to 150 MeV leads to small values of the real central proton optical potential strength, but does not significantly influence the distribution shapes shown in these figures. No attempt was made to explore in detail other refinements or parametrizations in these calculations since the major purpose of the present

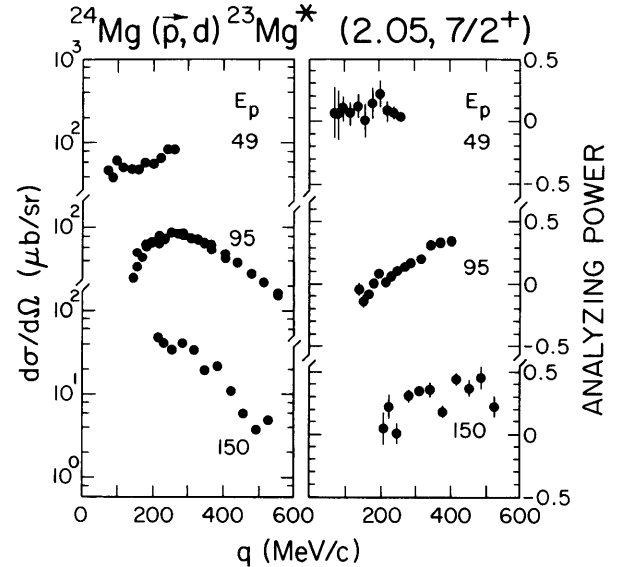


Figure 3. (p,d) differential cross section and analyzing-power angular distributions for the transition to the low-lying $7/2^+$ state in ^{23}Mg .

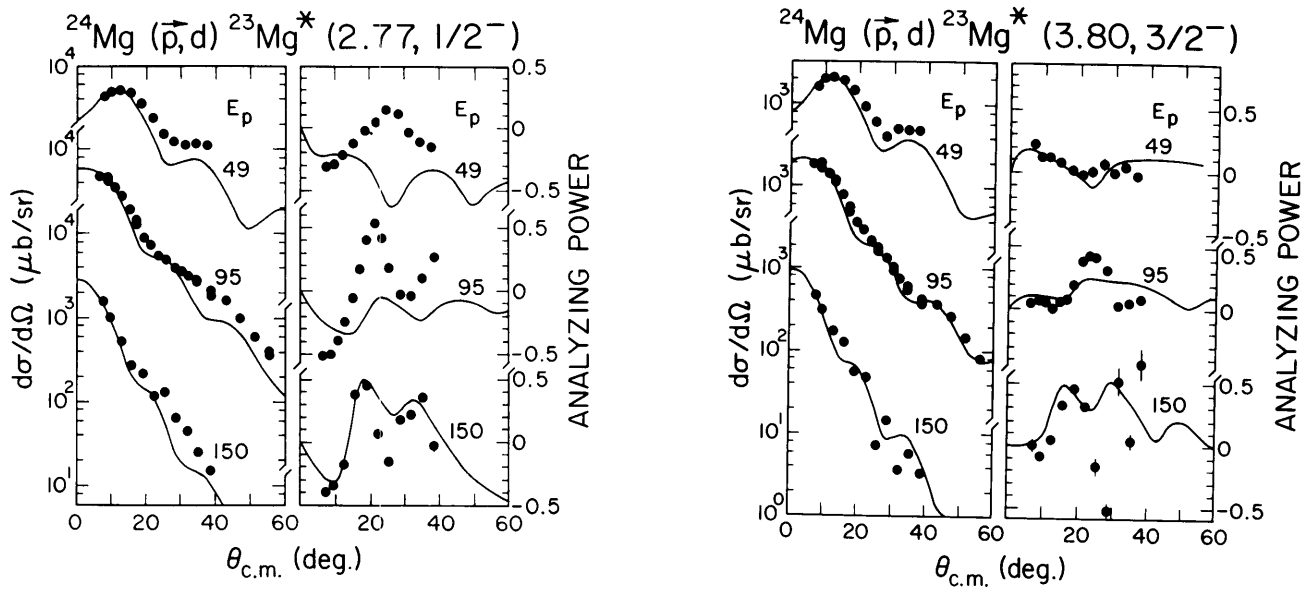


Figure 4. Comparison of cross-section and analyzing-power results at three bombarding energies for $\ell = 1$ (p,d) transitions with EFR distorted-wave calculations as described in text.

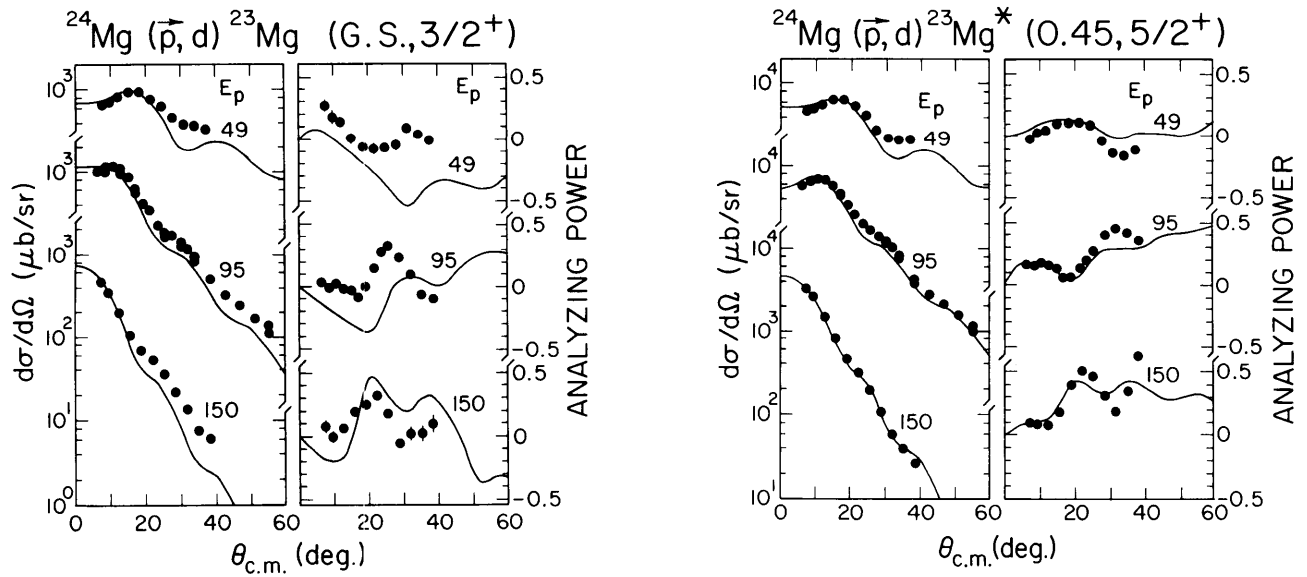


Figure 5. Comparison of cross-section and analyzing-power results at three bombarding energies for $\ell = 2$ (p,d) transitions with EFR distorted-wave calculations as described in text.

study was to provide the data base for future analyses of this type. However, substantial shortcomings are already apparent in the comparisons made here. For example, the analyzing powers for the $j = \ell-1/2$ cases are out-of-phase with the predictions at 49 MeV, but become in phase (though only roughly similar to the predictions) at the higher bombarding energies. The analyzing-power comparisons for the $j = \ell+1/2$ cases are generally better for all three energies, except for the 150-MeV result for the $3/2^-$ state at 3.80 MeV.

Spectroscopic factors extracted from a "correct" analysis should be independent of bombarding energy. The limited comparisons described above show an increase in the spectroscopic factors by a factor of 2 to 3 for the two $\ell = 0$ cases studied between 49 and 150 MeV. Only a small increase (30-50%) was observed in the spectroscopic factor over this energy range for the $\ell = 1$ cases studied, and the $\ell = 2$ comparisons showed that the extracted spectroscopic factor was essentially constant. This general trend is consistent with the fact that the $\ell = 0$ transitions more generally seem to cause problems in the calculations due to the increased momentum mismatch and the difficulty of treating the

nuclear interior properly. It should be noted that the more extensive analysis of Alons et al.⁴ of the $\ell = 0$ data show essentially no energy dependence of the spectroscopic factor from 27 to 185 MeV when a somewhat larger and more diffuse bound-state geometry is used, and impulse approximation optical-model parameters are employed at 150 and 185 MeV.

[†]Present address: Physics Department, Princeton University, Princeton, NJ 08544

- 1) J.R. Shepard, E. Rost, and P.D. Kunz, Phys. Rev. C 25, 1127 (1982).
- 2) D.W. Miller, W.P. Jones, D.W. Devins, R.E. Marrs, and J. Kehayias, Phys. Rev. C 20, 2008 (1979).
- 3) D.W. Miller, W.W. Jacobs, D.W. Devins, and W.P. Jones, Phys. Rev. C 26, 1793 (1982).
- 4) P.W.F. Alons, J.J. Kraushaar, D.W. Miller, J. Brown, D.L. Friesel, W.W. Jacobs, W.P. Jones, H. Nann, and P. Pichardo, Phys. Lett. 145B, 34 (1984).
- 5) H. Nann, D.W. Miller, W.W. Jacobs, D.W. Devins, W.P. Jones, and Li Qing-Li, Phys. Rev. C 27, 1073 (1983).
- 6) Program DWUCK5, P.D. Kunz (unpublished); extended version of J.R. Comfort (unpublished).
- 7) R.C. Johnson and P.J.R. Soper, Phys. Rev. C 1, 976 (1970); J.D. Harvey and R.C. Johnson, *ibid.* C 3, 636 (1971).
- 8) K. Hatanaka, M. Fujiwara, K. Hosono, N. Matsuoka, T. Saito and H. Sakai, Phys. Rev. C 29, 13 (1984).